

Spatiotemporal Distribution of Connexin45 in the Olivocerebellar System

RUBEN S. VAN DER GIESSEN,^{1*} STEPHAN MAXEINER,² PIM J. FRENCH,^{1,3}
KLAUS WILLECKE,² AND CHRIS I. DE ZEEUW¹

¹Department of Neuroscience, Erasmus MC, 3000 DR Rotterdam, The Netherlands

²Institut für Genetik, Abteilung Molekulargenetik, Universität Bonn,
D-53117 Bonn, Germany

³Department of Neurology, Erasmus MC, 3000 DR Rotterdam, The Netherlands

ABSTRACT

The olivocerebellar system is involved in the transmission of information to maintain sensory motor coordination. Gap junctions have been described in various types of neurons in this system, including the neurons in the inferior olive that provide the climbing fibers to Purkinje cells. While it is well established that Connexin36 is necessary for the formation of these neuronal gap junctions, it is not clear whether these electrical synapses can develop without Connexin45. Here we describe the development and spatiotemporal distribution of Connexin45 in relation to that of Connexin36 in the olivocerebellar system. During development Connexin45 is expressed in virtually all neurons of the inferior olive and cerebellar nuclei. During later postnatal development and adulthood there is a considerable overlap of expression of both connexins in subpopulations of all main olivary nuclei and cerebellar nuclei as well as in the stellate cells in the cerebellar cortex. Despite this prominent expression of Connexin45, ultrastructural analysis of neuronal gap junctions in null-mutants of Connexin45 showed that their formation appears normal in contrast to that in knockouts of Connexin36. These morphological data suggest that Connexin45 may play a modifying role in widely distributed, coupled neurons of the olivocerebellar system, but that it is not essential for the creation of its neuronal gap junctions. *J. Comp. Neurol.* 495:173–184, 2006.

© 2006 Wiley-Liss, Inc.

Indexing terms: Connexin36; inferior olive; cerebellar nuclei; cerebellar cortex; development; gap junctions; stellate cells

Gap junctions are protein complexes made up of several Connexins (Cx) that allow intercellular passage of signaling molecules or mono/divalent ions. Six connexin proteins cluster together to form a connexon or hemichannel and the docking of two hemichannels located in opposing membranes leads to the generation of functional gap junctions between neighboring cells (Kumar and Gilula, 1996). Homomeric connexons are composed of similar connexins, whereas heteromeric connexons consist of different connexins. Gap junctions formed by corresponding connexons are defined as homotypic channels, whereas heterotypic channels consist of different connexons. The number of possible interactions between various connexins therefore markedly increases the complexity of gap junctions. Specific connexin compositions result in different functional properties. For example, differences in permeability, affinity (Weber et al., 2004), and coupling asymmetry (Bev-

ans et al., 1998; Bukauskas et al., 2002) have been described. The connexin family includes at least 20 members in the murine genome and 21 connexin genes in the human genome (Willecke et al., 2002).

Grant sponsor: European Union; Grant sponsor: Nederlandse Organisatie voor Wetenschappelijk Onderzoek; Grant sponsor: Persoonsgerichte Impuls voor Onderzoeksgroepen met Nieuwe Ideeën voor Excellente Research (ZON-MW) (all to the laboratory of C.I.D.Z.); Grant sponsor: German Research Association; Grant number: Wi270/22-5,6 (Bonn laboratory, to K.W.).

*Correspondence to: Ruben Van Der Giessen, Department of Neuroscience, Erasmus MC, Dr. Molewaterplein 60, 3000 DR Rotterdam, The Netherlands. E-mail: r.vandergiesen@erasmusmc.nl

Received 30 March 2005; Revised 29 June 2005; Accepted 1 October 2005
DOI 10.1002/cne.20873

Published online in Wiley InterScience (www.interscience.wiley.com).

Only 10 of these connexin genes are expressed in the nervous system. While Cx57 appears to be specifically expressed in horizontal cells in the retina (Hombach et al., 2004), Cx26, Cx29, Cx30, C32, Cx43, and Cx47 have been found to be expressed in astrocytes and oligodendrocytes in the brain (Theis et al., 2005). Cx32 and Cx43 were originally suggested to be expressed by neurons in the central nervous system (Theis et al., 2003), but analysis of transgenic mice with connexin-specific markers indicated that these outcomes were probably incorrect (Nelles et al., 1996; Theis et al., 2003; Duan et al., 2004). It wasn't until the late 1990s that Condorelli et al. (1998) cloned, guided by the distribution of dendritic lamellar bodies that can be associated with dendrodendritic gap junctions (De Zeeuw et al., 1995), the first truly neuronal connexin (Cx36) (see also Söhl et al., 1998). Indeed, the absence of Cx36 results in neurons in nonfunctional "gap junction-like" structures with an abnormal wide distance between the two adjacent membranes, whereas in glia cells it does not affect the ultrastructure of their gap junctions (De Zeeuw et al., 2003). More recently, another connexin was also found to be expressed in neurons, without being expressed in astrocytes and oligodendrocytes: Cx45 (Condorelli et al., 2003; Maxeiner et al., 2003; Söhl et al., 2004). At present, it is unclear, however, whether Cx45 is coexpressed with Cx36 by the same neurons, and if so, whether Cx45 and Cx36 are expressed during the same developmental stages. In addition, it remains to be elucidated whether Cx45 is also necessary for the formation of neuronal gap junctions.

One of the best areas to tackle these questions is the inferior olive, since here the density of neuronal gap junctions is probably higher than any other brain region (De Zeeuw et al., 1995), because here gap junctions can be readily identified under the electron microscope (Sotelo et al., 1974; De Zeeuw et al., 1989), and because here Cx36 is virtually ubiquitously expressed (Belluardo et al., 2000; De Zeeuw et al., 2003; Degen et al., 2004). Olivary neurons are coupled through gap junctions, which are located between dendritic spines within glomeruli. These coupled spines receive both an inhibitory GABAergic input from the hindbrain and a non-GABAergic excitatory input from various areas providing ascending and descending projections to the olive (De Zeeuw et al., 1989, 1998). Apart from the inferior olive, the olivocerebellar system may also show the formation of gap junctions in both cerebellar nuclei and cerebellar cortex, because in these regions Cx36 is also prominently expressed (Degen et al., 2004). However, neuronal gap junctions have not been demonstrated yet at the electron microscopic level in these areas. Thus, to further uncover the spatiotemporal distribution of Cx45 in the olivocerebellar system and to explore the possible role of this connexin in the formation of its neuronal gap junctions, we investigated Cx45 transgenic mouse mutants for LacZ labeling, applied in situ hybridization and reverse transcriptase polymerase chain reaction (RT-PCR) analysis using Cx45 probes in wildtypes, and examined all three major parts of the olivocerebellar system, i.e., the inferior olive, cerebellar nuclei, and cerebellar cortex at the electron microscopy level in both Cx45 null mutants and wildtype littermates. Since our first global studies of Cx45 indicated that its role may be particularly relevant during early postnatal development (Maxeiner et al., 2003), special emphasis was put on its distribution during this stage.

MATERIALS AND METHODS

In situ hybridization

Mice at ages of postnatal days (P)1, P8, P14, and P21 were anesthetized with Nembutal (75 mg/kg, i.p.) and brains were carefully removed, frozen on dry ice, and stored at -80°C . Fourteen- μm sections were cut on a cryostat, mounted on polylysine-coated glass slides, and stored at -80°C . Slides were fixed in 4% paraformaldehyde (5 minutes), acetylated in 1.4% triethanolamine, 0.25% acetic anhydride, and prehybridized (1 hour) in buffer (pH 7.4) containing 50% formamide, $5\times$ SSC, $5\times$ Denhardt's, 250 $\mu\text{g/ml}$ yeast tRNA (Sigma, St. Louis, MO), and 500 $\mu\text{g/ml}$ acid-alkali cleaved salmon testis DNA (Sigma). In situ hybridization was performed essentially as described by De Zeeuw et al. (2003). Briefly, sections were incubated overnight at 65°C in prehybridization buffer containing 100 ng/ml digoxigenin-UTP-labeled cRNA probes. Sense and antisense probes were generated against the full-length coding sequence of Cx45 and Cx36 (500 bp) using a DIG RNA labeling kit (Roche, Nutley, NJ) was then hydrolyzed in 40 mM NaHCO_3 , 60 mM Na_2CO_3 for 25 minutes at 60°C to generate fragments of ~ 300 nucleotides. Sections were then washed in $0.2\times$ SSC at 65°C (1 hour) and blocked in 0.1 M Tris, pH 7.5, 0.15 M NaCl, and 10% heat inactivated sheep serum (Sigma) for 1 hour at room temperature (RT). Alkaline phosphatase conjugated anti-digoxigenin antibodies (1:5,000, Roche) containing 1% heat inactivated sheep serum were added to the sections and incubated overnight at 4°C . Color reactions were performed in 0.1 M Tris, pH 9.5, 0.1 M NaCl, 50 mM MgCl_2 , 2 mM Levamisole (Sigma), 0.35 mg/ml nitro-blue tetrazolium (Roche), and 0.18 mg/ml 5-bromo-4-chloro-3-indolylphosphate (Roche). Reactions were terminated upon visual inspection (~ 18 hours) and mounted in Permount (Fisher Scientific, Houston, TX). Cells were identified and quantified with the use of Neurolucida software. Labeled cells were counted and surface areas of these nuclei were measured. The outcomes of different slides per nucleus were averaged to a mean cell density (cells per mm^2) within the nuclei.

To confirm the in situ results obtained with the alkaline phosphatase method, we reexamined our findings using radioactive in situ hybridization. Brains from adult rats were removed, frozen on dry ice, and stored at -70°C . Fourteen- μm sections were cut on a cryostat, mounted onto polylysine-coated glass slides, and stored at -70°C . This form of in situ hybridization was performed essentially as described by French et al. (2001). Briefly, sections were thawed, fixed in 4% paraformaldehyde, acetylated in 1.4% triethanolamine and 0.25% acetic anhydride, dehydrated through graded ethanol solutions, and delipidated in chloroform. Sections were hybridized overnight at 42°C in 100 μl buffer (pH 7.0) containing 50% formamide, $4\times$ SSC, 10% dextran sulfate, $5\times$ Denhardt's solution, 200 mg/ml acid alkali cleaved salmon testis DNA, 100 mg/ml long-chain polyadenylic acid, 25 mM sodium phosphate (pH 7.0), 1 mM sodium pyrophosphate, and 100,000 CPM radiolabeled probe (~ 1 ng/ml) under parafilm coverslips. Sections were washed in $1\times$ SSC at 55°C (30 minutes), $0.1\times$ SSC at RT (5 minutes), and dehydrated in ethanol. Sections were then exposed to autoradiographic film. 35S-ATP end-labeled probes (NEN, Boston, MA) were generated using terminal deoxynucleotidyl transferase (Promega, Madison, WI) according to the manufacturer's

instructions. Either a 50-fold excess of unlabeled antisense oligonucleotide or the complementary sense oligonucleotide were used as negative controls. Sequences were: Connexin45 antisense 5'-ccatcaccacaaacaaccccc-3' and Connexin45 sense 5'-ggaagacacaacctgaaagttctgc-3'. Control sense oligos were complementary to the antisense oligo.

LacZ labeling

We used heterozygous Cx45-deficient mice with a mixed background of C57BL/6 and Sv129/Ola for LacZ-staining. These mice expressed the bacterial β -galactosidase protein under control of the endogenous Connexin45 promoter (Krüger et al., 2000). Connexin45 LacZ/+ mice were anesthetized with intraperitoneal Nembutal (75 mg/kg) and perfused transcardially with phosphate-buffered saline (PBS; pH 7.4) and 1% paraformaldehyde in 0.12 M PB. Whole brains were removed and postfixed in the same solution for 2 hours at room temperature. Brains were then transferred to 10% sucrose in 0.1 M PB at 4°C overnight and embedded in 11% gelatin and 10% sucrose in 0.1 M PB. Tissues were incubated in 30% sucrose and 10% formaldehyde solution at room temperature for 2 hours. Serial sections (40 μ m) were cut on a cryo modified sliding microtome (Leica, SM2000R) and collected in multiwells containing 0.1 M PB. Sections were incubated overnight with X-gal staining solution (PB, pH 7.4, supplemented with 5 mM $K_3[Fe(CN)_6]$, 5 mM $K_4[Fe(CN)_6]$, and 0.8% X-gal [5-bromo-4-chloro-3-indolyl- β -galactosidase]) at 37°C overnight. Subsequently, the 40- μ m sections were mounted and counterstained with neutral red to highlight the cellular localization of the blue X-gal staining, dehydrated, and embedded in Permount (Fisher Scientific).

To confirm the labeling pattern obtained with X-gal staining, we investigated the same regions using immunofluorescence. Cx45 LacZ/+ and wildtype mice were anesthetized by asphyxiation and sacrificed. Brains were then carefully removed, frozen on dry ice, and stored at -80°C. Sections (14 μ m) were cut on a cryostat, mounted on polylysine-coated glass slides, and stored at -80°C. Cryosections were fixed in 4% paraformaldehyde (30 minutes), rinsed in PBS, and incubated in 20 mM sodium citrate buffer (pH 8.7) at, respectively, 5 minutes 37°C, 5 minutes 60°C, and 3 hours 80°C. Sections were then blocked against endogenous peroxidase activity in PBS containing 0.5% H_2O_2 and 2% sodium azide. Sections were then transferred to blocking buffer (0.15% glycine and 0.5% Protifar in PBS, pH 7.6) for 30 minutes and incubated with β -galactosidase antibody (1:500, Abcam, Cambridge, UK) in blocking buffer overnight at 4°C. After incubation, samples were rinsed in blocking buffer and incubated for 90 minutes at RT in a concentration of 1:200 with secondary antibodies Alexa Fluor 594 goat antimouse (Molecular Probes, Leiden, The Netherlands) in blocking buffer. Sections were mounted in Vectashield kit containing DAPI (Vector Laboratories, Burlingame, CA) for nuclear staining.

RT-PCR analysis

Young wildtype mice at P1 and adult wildtype mice were anesthetized by asphyxiation in CO_2 and decapitated. Brains were carefully removed, frozen on dry ice, and stored at -80°C. The brainstem including the inferior olive, cerebellar nuclei, and cerebellar cortex was cut on a cryostat and stored at -80°C. The tissue was homogenized and RNA was extracted using the TRIzol procedure (Invitrogen, La Jolla, CA) according to the manufacturer's

instructions. The integrity of the RNA samples was checked on an agarose gel. cDNA was synthesized at 50°C (1 hour) using Superscript III reverse transcriptase (Invitrogen Life Technologies) and T18-oligo as the starting antisense primer. As control, reactions were performed without the addition of Superscript III reverse transcriptase. Using OD 260/280 nm measurements 0.1 μ g DNA out of each reverse transcriptase reaction was then used as template to amplify specific sequences in a PCR reaction containing 10 \times buffer (pH 9.0) with $MgCl_2$, 0.4 μ l dNTP, 0.4 μ l primers, and 0.5 μ l Taq DNA polymerase (Promega). Primers were: 5'-3': acttgaacacaccctctgc (Connexin45-sense primer), ttgtaggtccaatcgttcc (Connexin45-antisense primer), tctggagatgggtttctgc (Connexin36-sense primer), ggctacttgccactagcag (Connexin36-antisense primer), ctttgaccatctggatcg (Glucose-6-Phosphate Dehydrogenase-sense primer), cacttgacctctcatcaggac (Glucose-6-Phosphate Dehydrogenase-antisense primer). PCR was performed for 30, 33, and 36 cycles under the following conditions: denaturation for 2 minutes at 95°C, (annealing for 45 seconds at 95°C), annealing for 45 seconds at 56°C, and polymerization for 1 minute at 72°C. After amplification, the PCR products were analyzed by agarose gel electrophoresis and quantified with the use of Typhoon scanner 9410 (Amersham, UK) and analyzed using Scion Image 4.0.2 (NIH Image, Bethesda, MD).

Electron microscopy

Adult Cx45flox/flox:Nestin-Cre mice of 87.5% C57BL/6 and 12.5% 129SV/Ola background, which are referred to as Cx45-/- mice, were generated as reported by Maxeiner et al. (2003). Cx45-/- mice and wildtype littermates were anesthetized with an overdose of Nembutal and transcardially perfused with 4% paraformaldehyde and 1% glutaraldehyde in 0.12 M cacodylate buffer (pH 7.4); the brainstem containing the inferior olive, cerebellar nuclei, and cerebellar cortex were then processed for electron microscopy as described previously (De Zeeuw et al., 1989). In short, 100- μ m-thick sections were cut on a vibratome, osmicated in OsO_4 , stained for 24 hours in tannic acid and uranyl acetate, dehydrated in dimethoxypropane, and embedded in Araldite. Subsequently, the various olivary subnuclei were identified on semithin sections, pyramids were made, and ultrathin sections were cut accordingly on a Reichert ultratome, counterstained with uranyl acetate and lead citrate, and examined with a Philips CM-100 electron microscope. The sections of the various tissue blocks were systematically screened per surface area and the gap junctions were identified and quantified. For our investigations of the cerebellar cortex we labeled the Purkinje cells using standard immunocytochemistry with calbindin antibodies (Sigma, Zwijndrecht, The Netherlands) to make sure that the identification of the sources of the dendrites was correct (Bastianelli, 2003). Electron micrographs and other photographs were stored with the use of Adobe PhotoShop 7.0 (San Jose, CA). If necessary, photographs were modified or adjusted by changing the brightness or contrast ratio in this program.

RESULTS

Expression of Cx45 as revealed by in situ hybridization

At P1, P8, and P14, Cx45 was found to be expressed by neurons in the inferior olive, cerebellar nuclei, and cere-

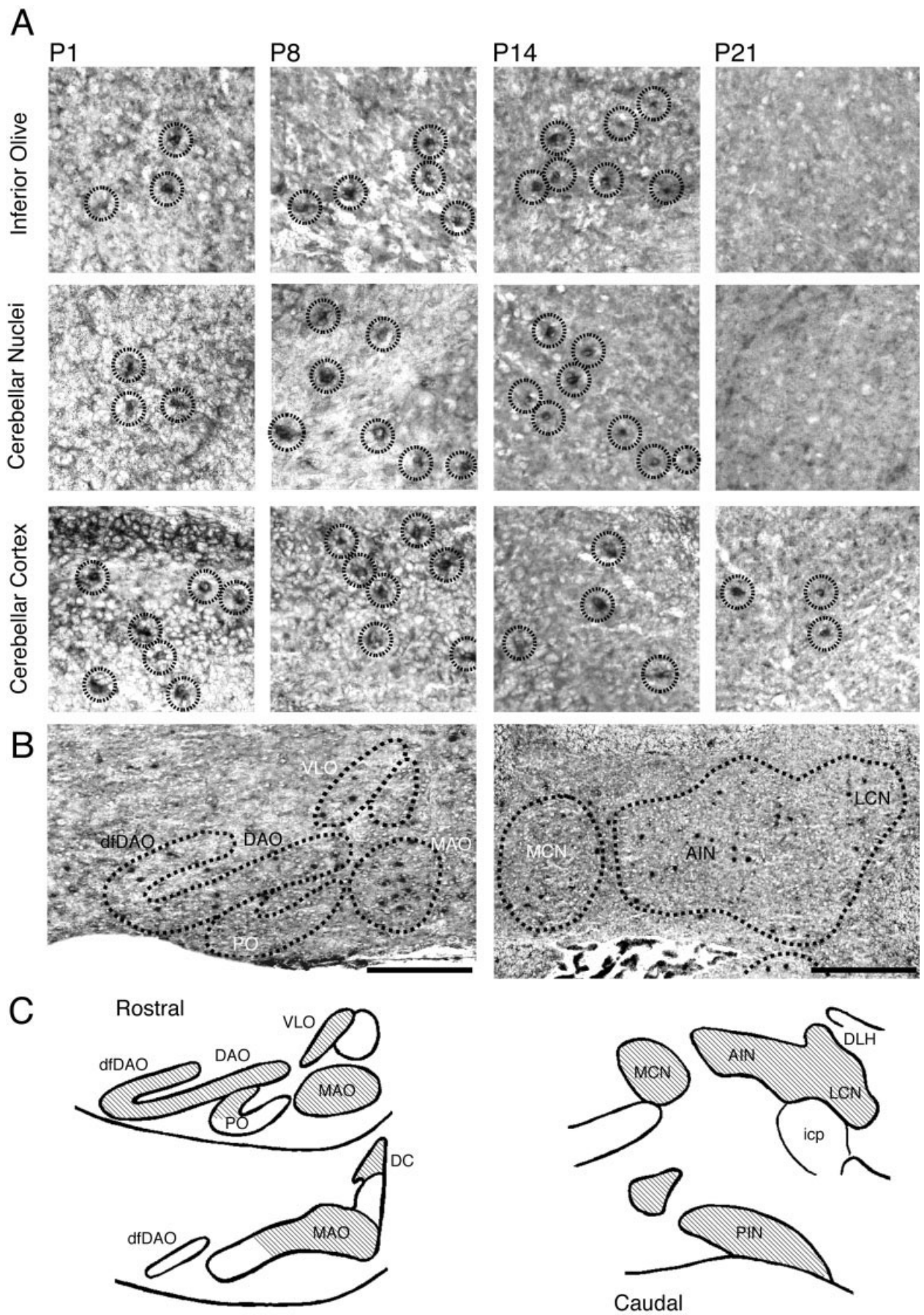


Figure 1

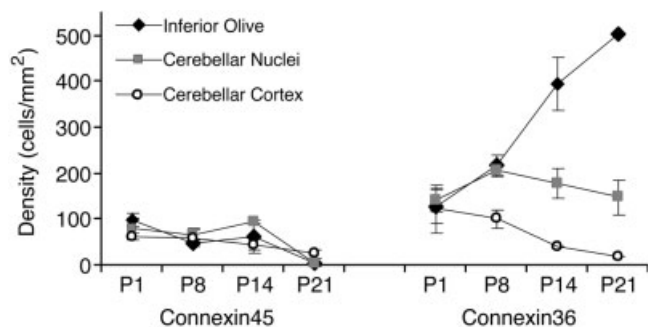


Fig. 2. Developmental expression of Connexin45 and Connexin36. Graphs show cell densities of brain areas expressing Cx45 or Cx36 during development based on cell counts after in situ hybridization. Labeled cells were counted and the surface areas of the nuclei were measured. Outcomes of different sections were averaged to a mean cell density within the brain region. Cx45 expression shows a decrease over time in all areas. Cx45-expressing cells mostly disappear at P21 except for the cerebellar cortex, which still shows labeled cells. In situ hybridization for Cx36 shows a massive increase in Cx36-expressing cells in the inferior olive, while in the cerebellar cortex cell numbers decrease during development. Results are shown as mean ± SD.

bellar cortex (Fig. 1A). During these periods of postnatal development the labeling in the inferior olive was mostly confined to the dorsal accessory olive (DAO) and medial accessory olive (MAO). In the cerebellar nuclei scattered labeled neurons were present in anterior interposed nucleus and posterior interposed nucleus (Fig. 1B,C), while in the cerebellar cortex the labeling was restricted to interneurons in the molecular layer. At ages of P21 and older only a few labeled neurons were observed in the inferior olive and cerebellar nuclei, and at a somewhat higher level in the cerebellar cortex (Fig. 2). Even though the numbers of labeled cells in these regions were relatively small, their presence persisted throughout adulthood.

For comparison we also quantified the number of labeled cells following in situ hybridization with the use of Cx36 probes (Fig. 2) (for raw material, see Degen et al., 2004). In the inferior olive the density of neurons expressing Cx36 showed, in contrast to those expressing Cx45, a large and steady increase starting at P1, while a relatively high saturated level persisted into adulthood. However, the density of Cx36-positive cells in the cerebellar nuclei and cerebellar cortex gradually diminished over time (Fig.

2). Ultimately, the densities of positively labeled neurons in both the nuclei and cortex reached a low but present level in the adult.

Expression of Cx45 as revealed by LacZ labeling

During early postnatal development (P1, P8, and P14) the spatial pattern of β-galactosidase-activity in the olivocerebellar system of Cx45LacZ/+ mice largely mimicked that obtained with in situ hybridization described above (data not shown). Yet during adulthood the sensitivity of LacZ labeling was generally higher than that of in situ hybridization, in that the densities of labeled neurons were higher (Figs. 3–5). In the inferior olive we found labeling at all rostrocaudal levels including the caudal MAO (b and c subnucleus), dorsal cap, dorsal and ventral leaf of the DAO, dorsal leaf of the principal olive (PO), ventrolateral outgrowth (VLO), and dorsomedial cell column (DMCC) (Fig. 3). Other parts such as the ventral leaf of the PO, beta-nucleus and rostral MAO hardly showed any labeled cell. The distribution of labeling that we observed in the inferior olive using immunofluorescence against β-galactosidase corresponded to that obtained with X-gal staining (compare Fig. 3B,C).

In the cerebellar nuclei we also observed X-gal staining in all their major subnuclei, including the lateral cerebellar nucleus, medial cerebellar nucleus, and anterior and posterior interposed nuclei (Fig. 4). Moreover, we found labeling in both the dorsal lateral protuberance and dorsal lateral hump. Yet parts of the medial cerebellar nucleus and posterior interposed nucleus as well as the entire lateral vestibular nucleus were devoid of labeling. Here, too, the labeling that we observed using immunofluorescence against β-galactosidase corresponded to that obtained with X-gal staining (compare Fig. 4C,D). This correspondence did not only hold for the precise distribution of the subnuclei involved, but also for the differences in densities observed among the various subnuclei (for differences in high and low densities, see distributions indicated by dark and light blue in Figs. 3 and 4, respectively). In addition, we observed many labeled interneurons in the molecular layer of the cerebellar cortex both during early postnatal development and adulthood (Fig. 5A). In fact, after P21 it was hard to find a single stellate cell in the molecular layer that was not positively labeled (Fig. 5B). In contrast, in the granular layer only few positively labeled cells were observed, while in the Purkinje cell layer no labeling was found at all.

One might argue that the LacZ labeling described above can be partly false-positive due to a long half-life of the β-galactosidase-protein, which is not endogenous. However, we found several areas in the brainstem such as the cuneate nucleus and the lateral reticular nucleus that showed abundant labeling during development, but hardly any labeling during adult stages (data not shown). Thus, false-positive labeling patterns are unlikely to persist for long periods as a general pattern, and we conclude that the LacZ labeling can result in not more than a modest overestimation in time.

Expression of Cx45 as revealed by RT-PCR analysis

Still, because the β-galactosidase staining and in situ hybridization cannot be used as quantitative methods and because the LacZ labeling in the adult appeared somewhat more dense than the labeling obtained with in situ

Fig. 1. In situ hybridization of Connexin45. **A:** Labeled neurons are shown in the inferior olive, cerebellar nuclei, and cerebellar cortex at P1, P8, P14, and P21. At P14, labeling of neurons is largely absent in the inferior olive and cerebellar nuclei, while in the cerebellar cortex labeling persists, although fewer cells are labeled. Dashed circles indicate labeled neurons. **B:** Inferior olive and cerebellar nuclei show labeling of Cx45-expressing cells at P14. **C:** Schematic drawing showing the Cx45 distribution at P14. Striped areas represent subnuclei where labeled neurons were found after in situ hybridization. Subnuclei are marked as positive when one or more labeled neurons were found. DAO, dorsal accessory olive; MAO, medial accessory olive; PO, principal olive; DM, dorsomedial group of PO; DMCC, dorsomedial cell column; dfDAO, dorsal fold of DAO; VLO, ventrolateral outgrowth; DC, dorsal cap; PIN, posterior interposed nucleus; MCN, medial cerebellar nucleus; LCN, lateral cerebellar nucleus; AIN, anterior interposed nucleus; DLH, dorsolateral hump; icp, inferior cerebellar peduncle. Scale bars = 100 μm in B (applies A,B).

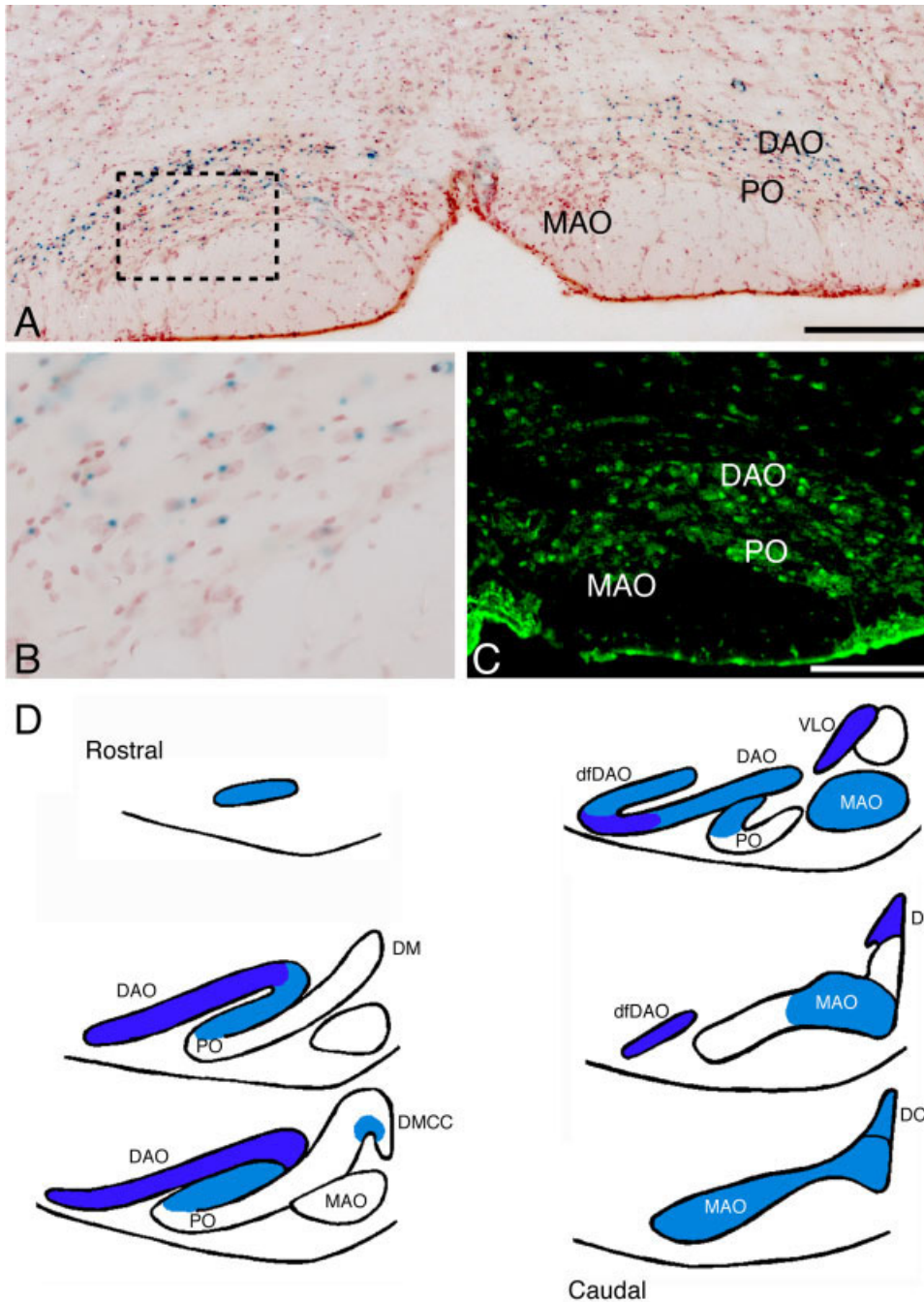


Fig. 3. Connexin45 LacZ-staining in the inferior olive. **A:** LacZ staining in the inferior olive reveals prominent labeling in the dorsal accessory olive and principal olive. **B:** Higher magnification showing LacZ-staining present in olivary neurons. **C:** Distribution of LacZ-expression in the inferior olive of Cx45-LacZ mice with the use of immunofluorescence. Immunolabeling of olivary neurons with anti- β -galactosidase antibodies depicts a pattern that resembles the LacZ-staining. **D:** Schematic drawing of LacZ-distribution in the inferior olive. The deep blue – light blue color gradients reflect high and low densities of LacZ-stained neurons, respectively. LacZ labeling is not present in the ventral leaf of principal olive and rostral part of the medial accessory olive. DAO, dorsal accessory olive; MAO, medial accessory olive; PO, principal olive; DM, dorsomedial group of PO; DMCC, dorsomedial cell column; dfDAO, dorsal fold of DAO; VLO, ventrolateral outgrowth; DC, dorsal cap. Scale bar = 100 μ m in A,C (applies to B,C).

hybridization, we used RT-PCR analysis as an additional semiquantitative method to compare the expression level of Cx45 in the olivocerebellar system of P1 with that of the adult. The RT-PCR data followed the outcomes of the LacZ labeling in that Cx45 was indeed still expressed in all parts of the olivocerebellar system during adulthood, but it followed the in situ results in that its expression in the inferior olive was significantly decreased from $60 \pm 1\%$ to $15 \pm 3\%$ during transition into adulthood ($P < 0.01$, *t*-test), while in the cortex it did not ($96 \pm 4\%$ vs. $83 \pm 15\%$) (Fig. 6). Expression in the cerebellar nuclei was also

significantly reduced (from $65 \pm 5\%$ to $45 \pm 3\%$; $P < 0.01$, *t*-test). The RT-PCR data obtained with Cx36 probes that were studied for control also correlated reasonably well with the histochemical data; the expression of Cx36 in the inferior olive increased from $73 \pm 5\%$ at P1 to $124 \pm 6\%$ in the adult ($P < 0.01$; *t*-test), while that in the cerebellar nuclei and cerebellar cortex decreased significantly (from $93 \pm 7\%$ to $47 \pm 2\%$ and from $105 \pm 7\%$ to $86 \pm 2\%$, respectively; $P < 0.01$ in both cases, *t*-test). Thus, taken together the RT-PCR data suggest that the higher sensitivity of the LacZ staining combined with the transient trends visible in the in situ

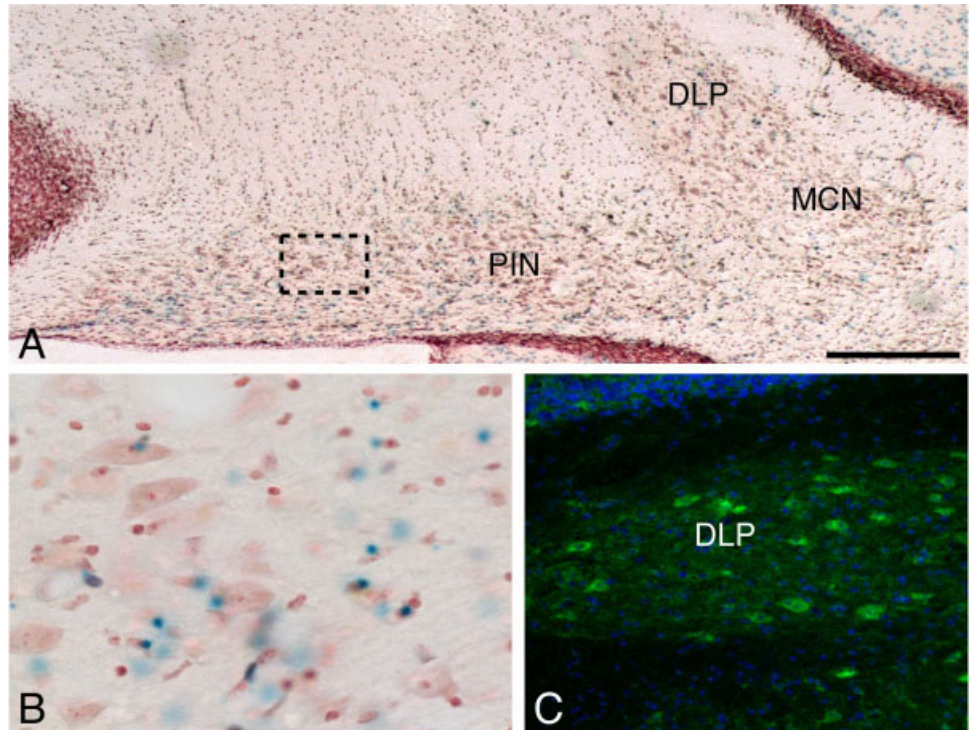
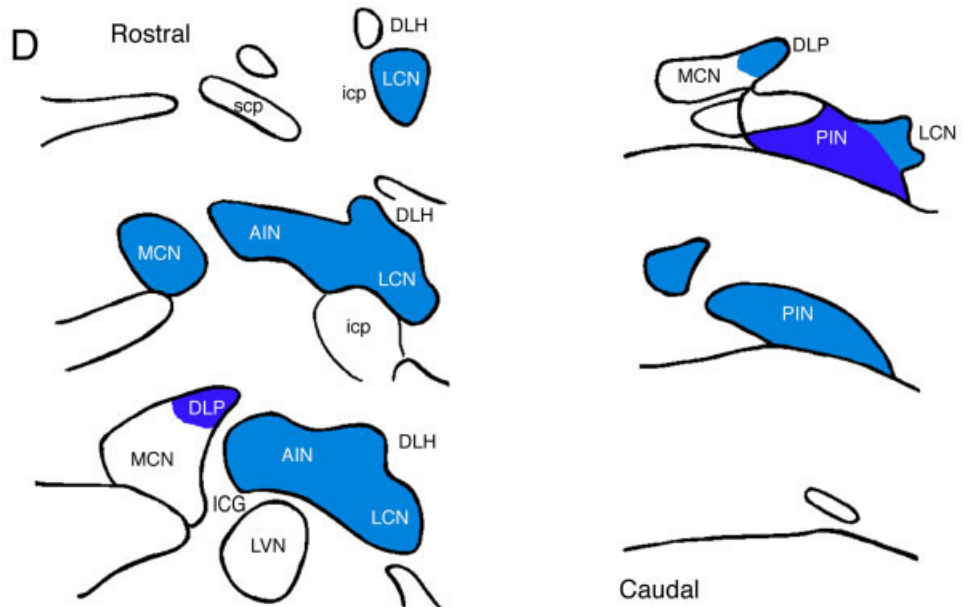


Fig. 4. Connexin45 LacZ staining in the cerebellar nuclei. **A:** LacZ staining shows strong labeling in the posterior interposed nucleus and dorsal lateral hump. **B:** Higher magnification from A showing labeling of the cerebellar nuclei neurons. **C:** The dorsolateral protuberance demonstrates immunolabeling of larger cerebellar nuclei neurons with the use of anti- β -galactosidase antibodies. **D:** Schematic drawing of the LacZ distribution the cerebellar nuclei. The deep blue – light blue color gradients reflect high and low densities of LacZ stained neurons, respectively. PIN, posterior interposed nucleus; DLP, dorsolateral protuberance; MCN, medial cerebellar nucleus; LCN, lateral cerebellar nucleus; LVN, lateral vestibular nucleus; AIN, anterior interposed nucleus; ICG, interstitial cell groups; DLH, dorsolateral hump; icp, inferior cerebellar peduncle; scp, superior cerebellar peduncle. Scale bar = 20 μ m in A (applies to A–D).



studies provide a reliable view for the spatiotemporal distribution of the expression of Cx45.

Electron microscopic analysis of neuronal gap junctions

It is clear from the data described above that even though Cx45 is most prominently present in the olivocerebellar system during early postnatal stages, it is still expressed at low levels in the inferior olive, cerebellar nuclei, and cerebellar cortex of the adult. These findings raise the question as to whether neuronal gap junctions do

not only occur within the inferior olive (Sotelo et al., 1974; De Zeeuw et al., 2003), but also between neurons in the cortex or nuclei. Thus, we set out experiments in wildtypes to find out whether neuronal gap junctions do occur between neurons in the cerebellum. In the cerebellar cortex of wildtypes we indeed found a substantial amount of dendrodendritic gap junctions (Fig. 7). In several cases one could reasonably distinguish the characteristic morphology of dendrites of stellate cells from that of Purkinje cells, but frequently we were unable to do so with sufficient certainty. We therefore labeled the Purkinje cell

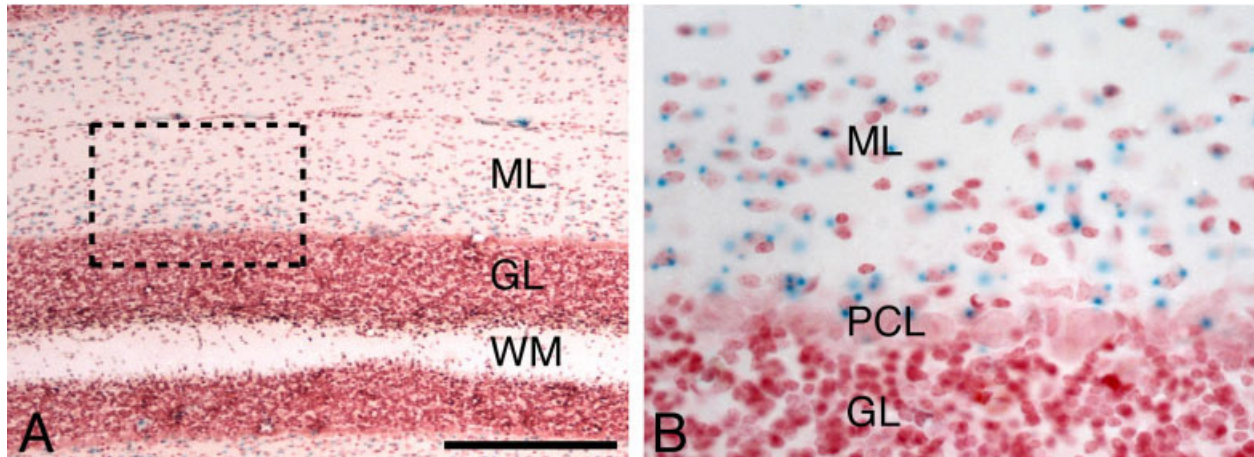


Fig. 5. Connexin45 LacZ-staining in the cerebellar cortex. **A:** LacZ-labeling in the cerebellar cortex was mostly restricted to the molecular layer. **B:** A higher magnification of A shows labeling of interneurons in

the cerebellar cortex. Notice abundant labeling present in almost every interneuron. ML, molecular layer; GL, granular layer; WM, white matter; PCL, Purkinje cell layer. Scale bar = 100 μm in A (applies to A,B).

dendrites with immunocytochemistry for calbindin and reexplored the cerebellar cortex. In this material, it was evident that all neuronal gap junctions in the cerebellar cortex occurred between stellate cells. The density of these gap junctions equaled 1 gap junction per 230,000 μm^2 of cerebellar cortex area. In contrast, in the cerebellar nuclei we did not find neuronal gap junctions with clear heptalaminar structures. We scanned more than a total area of 2,100,000 μm^2 , but were unable to detect a single gap junction embedded in the membranes of neuronal somata, dendrites, or axons in these regions. This lack does not appear to be an artifact in the technical preparation of the material, because we found a high number of glial gap junctions within the cerebellar nuclei, which were easily recognized.

Subsequently, we investigated the morphology and density of gap junctions in the neuropil of null-mutants of Cx45. In both the inferior olive and cerebellar cortex the gap junctions appeared totally normal with respect to their location in the neuropil as well as their morphology (Fig. 8A, top micrographs). We did not observe any significant difference in the average interneuronal distance (3.05 ± 0.3 nm in wildtype and 3.02 ± 0.7 nm in Cx45 $^{-/-}$ mice), plaque length (221 ± 47 vs. 220 ± 27 nm), interattachment distance (428 ± 53 vs. 436 ± 77 nm), or amount of electron-dense material on both cytoplasmic sides of the plaque among wildtypes and Cx45 knockouts. Moreover, the densities of gap junctions in the Cx45 knockout mice did not differ from those in wildtypes, neither in the inferior olive ($P > 0.25$; *t*-test) nor in the cerebellar cortex ($P > 0.5$; *t*-test). In this respect the Cx45 knockouts differed completely from the Cx36 null mutants, in which all normal gap junctions in the inferior olive have been found to turn into “gap junction-like” structures with abnormally spatially separated membranes (Fig. 8A, bottom micrographs) (for further details, see also De Zeeuw et al., 2003). Similarly, when we scanned more than 1,600,000 μm^2 in multiple slices of the cerebellar cortex of Cx36 $^{-/-}$ mice for gap junctions between stellate cells in the present study, we got the same result: No normal gap junctions were detected between stellate cells in these mice. Thus,

since Cx45 $^{-/-}$ mice show, in contrast to Cx36 $^{-/-}$ mice, normal gap junctions both between inferior olivary neurons and between stellate cells, Cx45 does not seem to be essential for the formation of neuronal gap junctions in the olivocerebellar system.

DISCUSSION

The major findings of the present study on the spatiotemporal distribution of Cx45 in the olivocerebellar system are that 1) Cx45 is expressed most prominently during early development; 2) Cx45 is expressed during adulthood but at relatively low levels; 3) Cx45 occurs in specific subnuclei of the inferior olive and cerebellar nuclei as well as interneurons of the molecular layer of the cerebellar cortex; and 4) Cx45 is not necessary for the structural formation of neuronal gap junctions in these regions. Below we discuss the spatiotemporal distribution of Cx45 for each of the three brain regions investigated, i.e., the inferior olive, cerebellar nuclei, and cerebellar cortex.

Inferior olive

Both the in situ hybridization and LacZ labeling methods showed that Cx45 is particularly prominently expressed in the inferior olive during early postnatal development. In fact, its expression even occurs slightly before the predecessors of normal gap junctions, i.e., the so-called “kissing junctions,” as well as the concomitant expression of Cx36 occur in the inferior olive (between P10 and P15, see Bourrat and Sotelo, 1983; Degen et al., 2004). This temporal order raises the possibility that Cx45 facilitates the initial creation of the neuronal gap junctions in the olivocerebellar system. This possibility is further supported by the finding that the spatial distribution of the expression of Cx45 during adulthood follows that of early postnatal development (compare Figs. 1C, 3D). However, at the same time it should be noted that not all olivary subnuclei expressed Cx45, while all neurons in all subnuclei do express Cx36 both during development and adulthood (De Zeeuw et al., 2003). Moreover, the morphological characteristics of the neuronal gap junctions in the Cx45

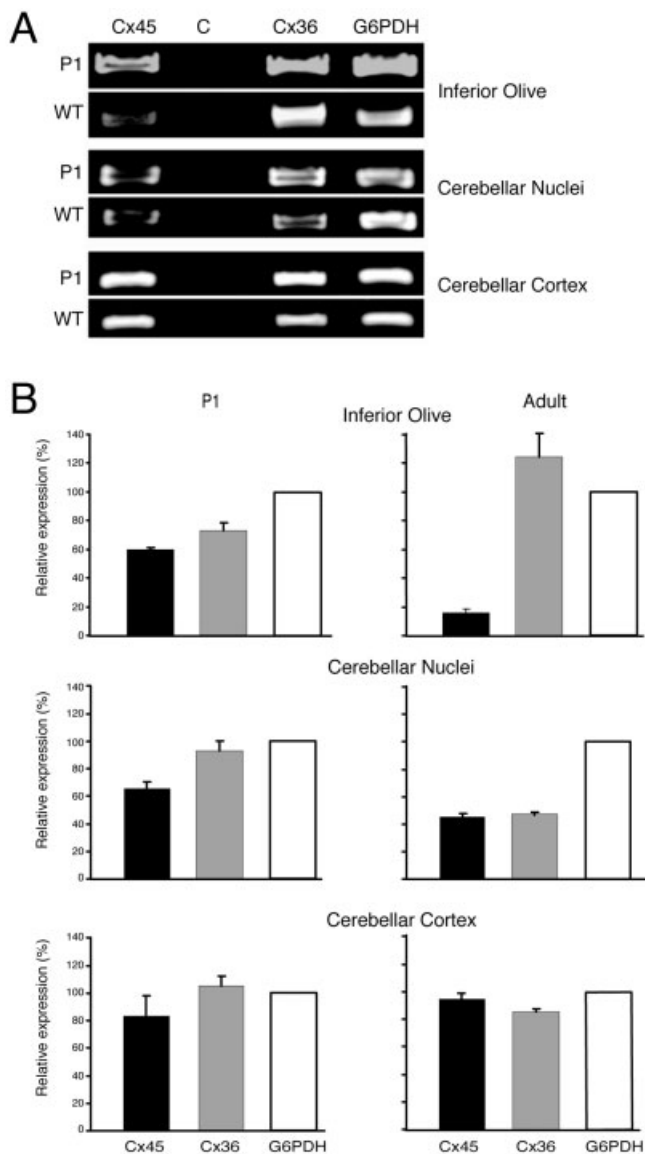


Fig. 6. Expression analysis of Connexin45 and Connexin36 using RT-PCR. RT-PCR analysis of P1 wildtype and adult wildtype mice, respectively. Negative control (C) is RT-PCR performed without Superscript III. **A:** Expression analysis of Cx45, Cx36, and G6PDH in inferior olive, cerebellar nuclei, and cerebellar cortex. **B:** Graphs of relative expression compared to G6PDH-expression. The inferior olive expression pattern shows a relative upregulation of Cx36 and a down-regulation of Cx45. In the cerebellar nuclei both Connexins show a decrease in expression, while in the cerebellar cortex the expression stays almost consistent throughout development. All results are shown as mean \pm SEM.

null-mutants appeared totally unaffected in contrast to those in Cx36 null-mutants. Thus, if Cx45 plays a role in the formation of neuronal gap junctions, it has to be limited to particular subsets of neurons and it has to be reflected by physiological parameters rather than structural characteristics.

Since all olivary cells express Cx36 (De Zeeuw et al., 2003), while only part express Cx45 during adulthood (present study), it is clear that the inferior olive does not

have any neuron that solely expresses Cx45. This finding raises the possibility that Cx45 may serve to modify the electrical properties of the neuronal gap junctions that are predominantly formed by Cx36. Such a possibility is supported by the fact that Cx45 contains phosphorylation sites, which can affect the conductance properties, and that Cx45 can form, apart from homomeric, also heteromeric or heterotypic gap junctions (Hertlein et al., 1998; van Veen et al., 2000; Valiunas, 2002; Maxeiner et al., 2005). Moreover, a subtle functional role of Cx45 is also in line with the observation that Cx45 itself cannot fully compensate for a lack of Cx36 (De Zeeuw et al., 2003). Thus, the expression of Cx45 in the adult mice might play a role in altering various functional properties of the gap junctions by forming protein complexes with other connexins in the inferior olive.

Cerebellar nuclei

The in situ hybridization experiments, the LacZ labeling experiments, as well as the RT-PCR analyses showed that Cx45 and Cx36 are both prominently expressed in various parts of all cerebellar nuclei both during development and adulthood. Even so, we have not been able to detect any neuronal gap junction in our electron microscopic examination. In some cases there was a hint of an axosomatic junction similar to structures described for the vestibular nuclei (Korn et al., 1973; De Zeeuw and Berrebi, 1995), but we have not been able to identify a clear heptalaminar structure in any of these membranous processes. Possibly, we and other electron microscopists of the cerebellar nuclei have failed to detect neuronal gap junctions because they may be extremely difficult to find (Van der Want et al., 1989). Perhaps the plaques in these nuclei are much smaller than in other regions and may be even harder to detect than those of glial gap junctions, which can also be readily observed in the cerebellar nuclei (present study). Alternatively, one might wonder whether the connexins expressed in the nuclei are being used at another place, for example, the inferior olive. One could speculate that the connexins are transported via the axons of the cerebellar GABAergic neurons to their terminals, which are indeed known to be located directly at the spines that are coupled by dendrodendritic gap junctions in the olivary glomeruli (De Zeeuw et al., 1989, 1998). Such a process could in fact be used as a mechanism to make sure that the vast majority of the olivary gap junctions are located at the peripheral spines that are strategically innervated by the GABAergic input from the nuclei. Interestingly, the subnuclei of the inferior olive that do not express Cx45, i.e., the ventral leaf of the PO and rostral MAO, do receive this GABAergic input from the cerebellar nuclei that prominently express Cx45, i.e., the lateral cerebellar nucleus and posterior interposed nucleus, respectively (present study; Ruigrok and Voogd, 2000). Thus, although this wild speculation reaches beyond the natural cell biological rule that proteins are used by the cells by which they are made, there are arguments and observations that are compatible with it.

Cerebellar cortex

Both the in situ hybridization experiments and the LacZ labeling experiments demonstrated that all interneurons in the molecular layer of the cerebellar cortex express Cx45 during both early postnatal development and adulthood. Guided by the labeling, we indeed showed for the

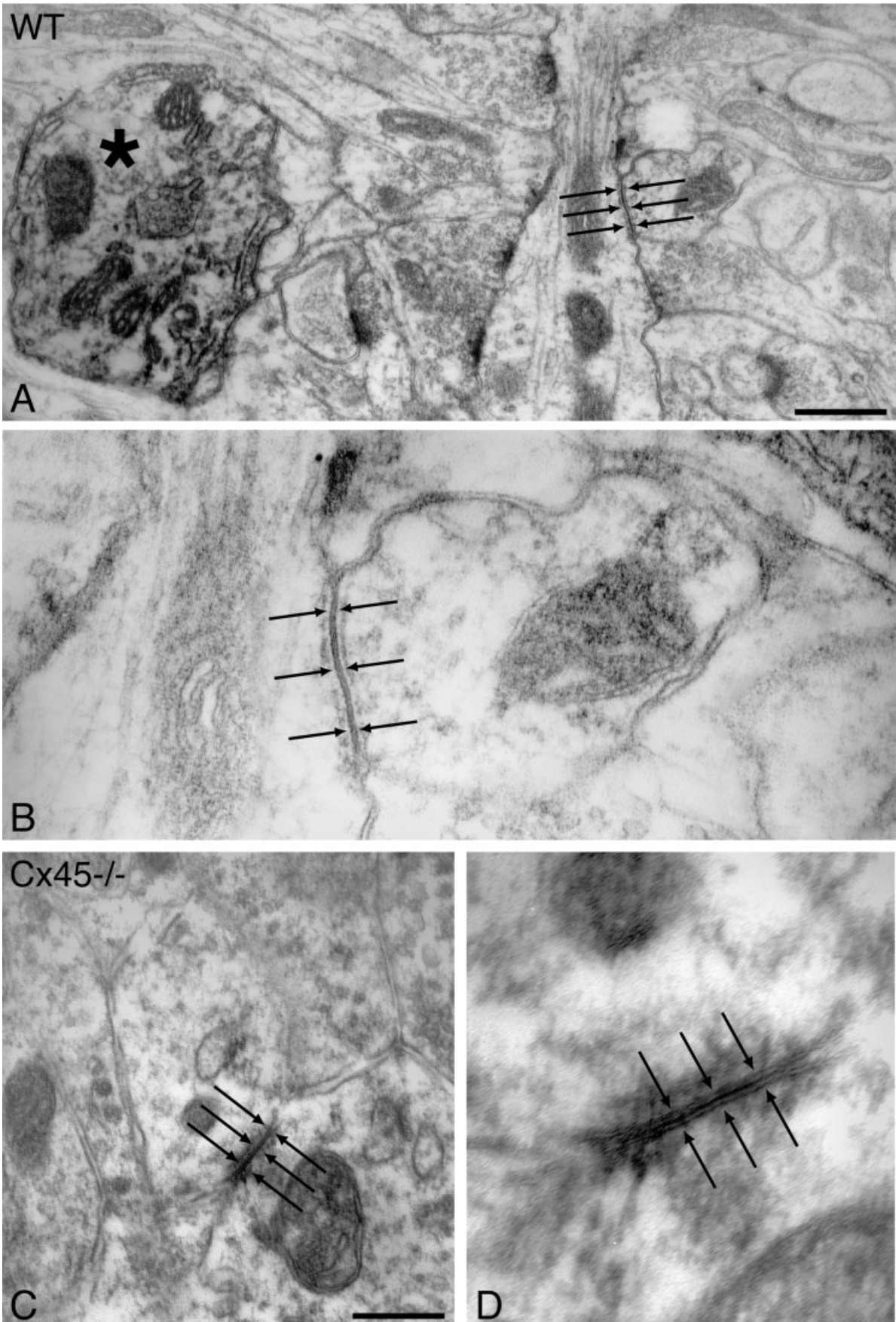


Fig. 7. Gap junctions between stellate cells in the cerebellar cortex. **A:** Ultrastructural micrograph shows a dendrodendritic gap junction between stellate cell dendrites in a wildtype mouse (see arrows). To distinguish the dendrites from Purkinje cells (marked by asterisk), immunocytochemistry for calbindin was used to label the Purkinje cell dendrites. **B:** Higher magnification of the dendrodendritic gap junction,

which shows a clear plaque with some dense material around the gap junction (plaque is indicated by arrows). **C:** A dendrodendritic gap junction (see arrows) between stellate cell dendrites in a Connexin45-deficient mouse. **D:** A higher magnification of a gap junction plaque (indicated by arrows) between stellate cells surrounded by dense material. Scale bars = 200 nm in A (applies to A,B), C (applies to C,D).

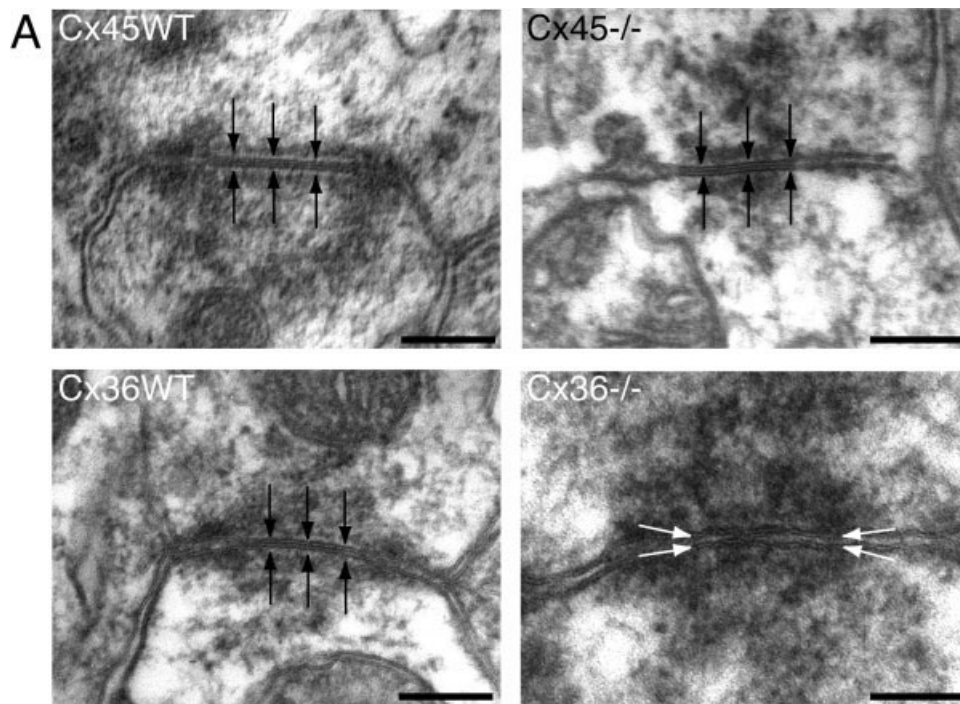
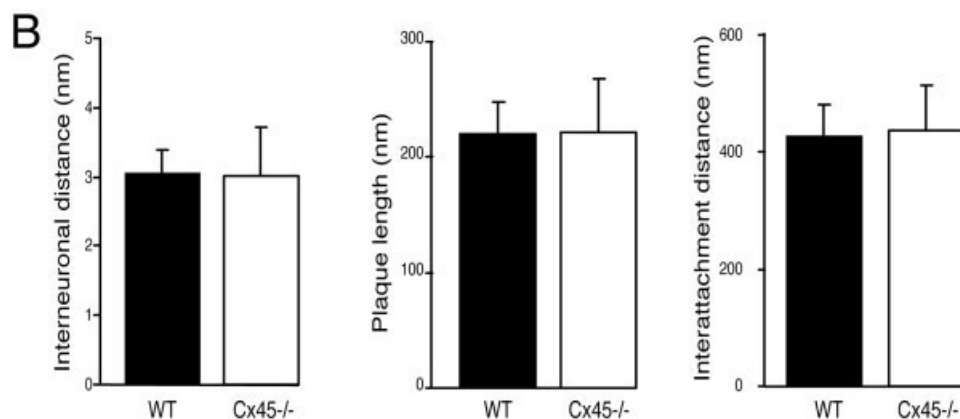


Fig. 8. Olivary gap junctions in inferior olive. **A:** Ultrastructural micrographs showing dendrodendritic gap junctions in the inferior olive of wildtype mice, Connexin45-deficient mice and Connexin36-deficient mice. In both the wildtype animals and Cx45-deficient mice normal gap junctions are found with a normal plaque (indicated by black arrows; see also histograms in **B**). In contrast gap junctions in the Cx36-deficient mutants show an increased interneuronal distance (indicated by white arrows). **B:** Histograms reveal the morphometric characteristics of gap junctions in wildtype and Cx45-deficient mice. The average interneuronal distance, plaque length, and interattachment distance were almost equal compared to the wildtype mice. All results are shown as mean \pm SD. Scale bars = 100 nm.



first time the existence of neuronal gap junctions between stellate cells. These data agree well with the cell physiological findings of Mann-Metzer and Yarom (1999, 2000), who demonstrated electrotonic coupling between inhibitory interneurons in the molecular layer within the cerebellar cortex. Yet in this region, too, the presence of Cx45 was not essential for the structural formation of neuronal gap junctions, as their morphology was not abnormal. Thus, similar to the inferior olive, Cx45 in the cerebellar cortex may serve a role so as to subtly modify the function of neuronal gap junctions, but it appears unlikely that it is necessary for the occurrence of electrotonic coupling itself.

LITERATURE CITED

Bastianelli E. 2003. Distribution of calcium-binding proteins in the cerebellum. *Cerebellum* 2:242–262.
 Belluardo N, Mudo G, Trovato-Salinaro A, Le Gurun S, Charollais A, Serre-Beinier V, Amato G, Haefliger JA, Meda P, Condorelli DF. 2000.

Expression of connexin36 in the adult and developing rat brain. *Brain Res* 865:121–138.
 Bevans CG, Kordel M, Rhee SK, Harris AL. 1998. Isoform composition of connexin channels determines selectivity among second messengers and uncharged molecules. *J Biol Chem* 273:2808–2816.
 Bourrat F, Sotelo C. 1983. Postnatal development of the inferior olivary complex in the rat. I. An electron microscopic study of the medial accessory olive. *Brain Res* 284:291–310.
 Bukauskas FF, Angele AB, Verselis VK, Bennett MV. 2002. Coupling asymmetry of heterotypic connexin 45/connexin 43-EGFP gap junctions: properties of fast and slow gating mechanisms. *Proc Natl Acad Sci U S A* 99:7113–7118.
 Condorelli DF, Parenti R, Spinella F, Trovato Salinaro A, Belluardo N, Cardile V, Cicerata F. 1998. Cloning of a new gap junction gene (Cx36) highly expressed in mammalian brain neurons. *Eur J Neurosci* 10:1202–1208.
 Condorelli DF, Trovato-Salinaro A, Mudo G, Mirone MB, Belluardo N. 2003. Cellular expression of connexins in the rat brain: neuronal localization, effects of kainate-induced seizures and expression in apoptotic neuronal cells. *Eur J Neurosci* 18:1807–1827.
 De Zeeuw CI, Berrebi AS. 1995. Postsynaptic targets of Purkinje cell

- terminals in the cerebellar and vestibular nuclei of the rat. *Eur J Neurosci* 7:2322–2333.
- De Zeeuw CI, Holstege JC, Ruigrok TJ, Voogd J. 1989. Ultrastructural study of the GABAergic, cerebellar, and mesodiencephalic innervation of the cat medial accessory olive: anterograde tracing combined with immunocytochemistry. *J Comp Neurol* 284:12–35.
- De Zeeuw CI, Hertzberg EL, Mugnaini E. 1995. The dendritic lamellar body: a new neuronal organelle putatively associated with dendrodendritic gap junctions. *J Neurosci* 15:1587–1604.
- De Zeeuw CI, Simpson JI, Hoogenraad CC, Galjart N, Koekkoek SK, Ruigrok TJ. 1998. Microcircuitry and function of the inferior olive. *Trends Neurosci* 21:391–400.
- De Zeeuw CI, Chorev E, Devor A, Manor Y, Van Der Giessen RS, De Jeu MT, Hoogenraad CC, Bijman J, Ruigrok TJ, French P, Jaarsma D, Kistler WM, Meier C, Petrasch-Parwez E, Dermietzel R, Söhl G, Gueldenagel M, Willecke K, Yarom Y. 2003. Deformation of network connectivity in the inferior olive of connexin 36-deficient mice is compensated by morphological and electrophysiological changes at the single neuron level. *J Neurosci* 23:4700–4711.
- Degen J, Meier C, Van Der Giessen RS, Söhl G, Petrasch-Parwez E, Urschel S, Dermietzel R, Schilling K, De Zeeuw CI, Willecke K. 2004. Expression pattern of lacZ reporter gene representing connexin36 in transgenic mice. *J Comp Neurol* 473:511–525.
- Duan L, Yuan H, Su CJ, Liu YY, Rao ZR. 2004. Ultrastructure of junction areas between neurons and astrocytes in rat supraoptic nuclei. *World J Gastroenterol* 10:117–121.
- French PJ, O'Connor V, Voss K, Stean T, Hunt SP, Bliss TV. 2001. Seizure-induced gene expression in area CA1 of the mouse hippocampus. *Eur J Neurosci* 14:2037–2041.
- Hertlein B, Butterweck A, Haubrich S, Willecke K, Traub O. 1998. Phosphorylated carboxy terminal serine residues stabilize the mouse gap junction protein connexin45 against degradation. *J Membr Biol* 162:247–257.
- Hombach S, Janssen-Bienhold U, Söhl G, Schubert T, Bussow H, Ott T, Weiler R, Willecke K. 2004. Functional expression of connexin57 in horizontal cells of the mouse retina. *Eur J Neurosci* 19:2633–2640.
- Korn H, Sotelo C, Crepel F. 1973. Electronic coupling between neurons in the rat lateral vestibular nucleus. *Exp Brain Res* 16:255–275.
- Krüger O, Plum A, Kim JS, Winterhager E, Maxeiner S, Hallas G, Kirchoff S, Traub O, Lamers WH, Willecke K. 2000. Defective vascular development in connexin 45-deficient mice. *Development* 127:4179–4193.
- Kumar NM, Gilula NB. 1996. The gap junction communication channel. *Cell* 84:381–388.
- Mann-Metzer P, Yarom Y. 1999. Electrotonic coupling interacts with intrinsic properties to generate synchronized activity in cerebellar networks of inhibitory interneurons. *J Neurosci* 19:3298–3306.
- Mann-Metzer P, Yarom Y. 2000. Electrotonic coupling synchronizes interneuron activity in the cerebellar cortex. *Prog Brain Res* 124:115–122.
- Maxeiner S, Krüger O, Schilling K, Traub O, Urschel S, Willecke K. 2003. Spatiotemporal transcription of connexin45 during brain development results in neuronal expression in adult mice. *Neuroscience* 119:689–700.
- Maxeiner S, Dedek K, Janssen-Bienhold U, Ammermuller J, Brune H, Kirsch T, Pieper M, Degen J, Krüger O, Willecke K, Weiler R. 2005. Deletion of connexin45 in mouse retinal neurons disrupts the rod/cone signaling pathway between AII amacrine and ON cone bipolar cells and leads to impaired visual transmission. *J Neurosci* 25:566–576.
- Nelles E, Butzler C, Jung D, Temme A, Gabriel HD, Dahl U, Traub O, Stumpel F, Jungermann K, Zielasek J, Toyka KV, Dermietzel R, Willecke K. 1996. Defective propagation of signals generated by sympathetic nerve stimulation in the liver of connexin32-deficient mice. *Proc Natl Acad Sci U S A* 93:9565–9570.
- Ruigrok TJ, Voogd J. 2000. Organization of projections from the inferior olive to the cerebellar nuclei in the rat. *J Comp Neurol* 426:209–228.
- Söhl G, Degen J, Teubner B, Willecke K. 1998. The murine gap junction gene connexin36 is highly expressed in mouse retina and regulated during brain development. *FEBS Lett* 428:27–31.
- Söhl G, Odermatt B, Maxeiner S, Degen J, Willecke K. 2004. New insights into the expression and function of neural connexins with transgenic mouse mutants. *Brain Res Brain Res Rev* 47:245–259.
- Sotelo C, Llinas R, Baker R. 1974. Structural study of inferior olivary nucleus of the cat: morphological correlates of electrotonic coupling. *J Neurophysiol* 37:541–559.
- Theis M, Söhl G, Speidel D, Kuhn R, Willecke K. 2003. Connexin43 is not expressed in principal cells of mouse cortex and hippocampus. *Eur J Neurosci* 18:267–274.
- Theis M, Söhl G, Eiberger J, Willecke K. 2005. Emerging complexities in identity and function of glial connexins. *Trends Neurosci* 28:188–195.
- Valiunas V. 2002. Biophysical properties of connexin-45 gap junction hemichannels studied in vertebrate cells. *J Gen Physiol* 119:147–164.
- Van der Want JJ, Wiklund L, Guegan M, Ruigrok T, Voogd J. 1989. Anterograde tracing of the rat olivocerebellar system with Phaseolus vulgaris leucoagglutinin (PHA-L). Demonstration of climbing fiber collateral innervation of the cerebellar nuclei. *J Comp Neurol* 288:1–18.
- van Veen TA, van Rijen HV, Jongsma HJ. 2000. Electrical conductance of mouse connexin45 gap junction channels is modulated by phosphorylation. *Cardiovasc Res* 46:496–510.
- Weber PA, Chang HC, Spaeth KE, Nitsche JM, Nicholson BJ. 2004. The permeability of gap junction channels to probes of different size is dependent on connexin composition and permeant-pore affinities. *Biophys J* 87:958–973.
- Willecke K, Eiberger J, Degen J, Eckardt D, Romualdi A, Gueldenagel M, Deutsch U, Söhl G. 2002. Structural and functional diversity of connexin genes in the mouse and human genome. *Biol Chem* 383:725–737.